GEOPHYSICAL RESEARCH LETTERS, VOL. 25, NO. 9, PAGES 1419-1422, MAY 1, 1998

Global variation of column droplet concentration in low-level clouds

Qingyuan Han[1], William B. Rossow[2], Joyce Chou[1] and Ronald M. Welch[1]

Abstract. Cloud droplet concentration is a very important parameter in model studies. However, no global observation is available because it is hard to retrieve by current satellite remote sensing techniques. This study introduces another parameter, column droplet concentration, which can be retrieved by satellite data and used in models. The column droplet concentration (N_c) is the product of cloud geometrical thickness and droplet volume number concentration. This paper presents a method and the results of retrieving column droplet concentration for low-level clouds. The first near-global survey (50°S to 50°N) of N_c reveals more clearly the effect of aerosol concentration variations on clouds. The survey shows the expected increase of column droplet concentrations between ocean and continental clouds and in tropical areas during dry seasons where biomass burning is prevalent. Therefore, column droplet concentration is demonstrated as a good indication of available CCN populations in certain areas.

1. Introduction

To study the effect on climate of anthropogenic changes of aerosol requires a coupled atmospheric chemistry-aerosol-cloud-climate model. The most significant uncertainties are the effects of clouds on aerosol formation and removal and the effects of changing aerosols on cloud properties. The most direct effect of aerosol on clouds is that the concentration of cloud condensation nuclei (CCN), that subset of aerosols that interact most effectively with water, determines the number density of droplets during cloud formation. Although a one-to-one correspondence between the number concentration of CCN (N_a) in the sub-cloud layer and the number concentration of cloud droplets (N) in clean maritime air masses has been reported [*Martin et al.*, 1994], usually only a small fraction of the aerosol is activated to become cloud droplets in other regions [*Raga and Jonas*, 1993]. Thus, the relationship between N_a and N is monotonic, though non-linear [*Jones et al.*, 1994]; but it may vary with location and season. It is realized that to better depict the cloud microphysical processes and feedbacks in climate models, observations of both droplet number concentration and droplet size are needed [*Schwartz and Slingo*, 1996]. In recent model studies, cloud properties other than N are assumed to be independent of changes in N_a. However, cloud geometrical thickness may actually change during aerosol-cloud interactions, which has been observed under both clear [*e.g.*, *Conover*, 1966] and cloudy [*e.g.*, *Hobbs et al.*, 1970] conditions. Thus, the effective droplet number concentration N used in climate models combines the effects of changes in geometrical thickness and changes in droplet number concentration, which is given by the changes in N_c, viz., $\Delta N_c/N_c=\Delta h/h + \Delta N/N$. In a GCM model, the predicted droplet number concentrations change substantially with vertical resolution [*Ghan et al.*, 1997]. In this paper, we show that the variable N_c can be retrieved from satellite radiance data and used to test model parameterizations.

[1]Department of Atmospheric Science, University of Alabama in Huntsville, Huntsville, AL.
[2]NASA Goddard Institute for Space Studies, New York, NY.

Copyright 1998 by the American Geophysical Union.

Paper number 98GL01095.
0094-8534/98/98GL-01095$05.00

2. Methodology

We retrieve cloud optical thickness (τ) and effective droplet radius (r_e) from satellite-measured radiances at 0.63, 3.7 and 10.7 μm wavelength (channels 1, 3 and 4 of AVHRR on NOAA polar orbiting satellites) by comparison with calculations from a radiative transfer model that represents the spectral and angle dependence of radiation, accounting for multiple scattering by gases and clouds and for other atmospheric and surface effects [*Han et al.*, 1994]. The analysis is applied to pixel-level data (called CX) from the International Satellite Cloud Climatology Project (ISCCP, *Rossow and Schiffer*, 1991) which identifies cloudy satellite pixels. Liquid water clouds are identified by channel 4 brightness temperatures > 273 K, implying cloud tops below the freezing level. Individual pixels are about 4 km across and have been sampled at intervals of about 30 km. Since cloud scattering at 0.63 μm is conservative, τ values represent the whole cloud layer; whereas, most of the signal at 3.7 μm used to determine r_e comes from the uppermost portion of the cloud [*Han et al.*, 1994]. See *Han et al.* (1995) for comparisons of these results with other measurements.

A review of literature on cloud microphysical processes shows that they depend on three main parameters from which all other quantities can be calculated [*Rossow*, 1978]: volume number density (N), mean particle size (since we consider only liquid water clouds here, we will henceforth use droplet radius, $\bar{r}$), and the thickness of the cloud layer (h). Aerosol characteristics and atmospheric dynamics (cooling rate) determine the number of nucleated droplets, N, which varies little unless collisional growth begins to form precipitation. We are neglecting changes in the droplet size distribution by representing it only by N and $\bar{r}$, even though the width of the size distribution affects precipitation formation, because precipitating clouds are relatively rare [*Lin and Rossow*, 1996]. The atmospheric dynamics and thermodynamics determine how much water is condensed from vapor, and thus, the cloud droplet size. They also determine the cloud vertical extent. Since variations of updraft strength (or cooling rate) with altitude can make LWC and $\bar{r}$ vary with altitude through the cloud layer, we interpret $\bar{r}$ to be the volume-averaged droplet size over the cloud layer, then average $LWC=(4/3)\rho_w\pi N\bar{r}^3$ and $LWP=LWC\cdot h=(4\pi/3)\rho_w\bar{r}^3N_c$.

The column droplet concentration is defined by

$$N_c=N\cdot h \tag{1}$$

Thus,

$$\frac{\Delta N_c}{N_c}=\frac{\Delta h}{h}+\frac{\Delta N}{N} \tag{2}$$

i.e., the relative change of N_c is equal to that of N if $\Delta h/h$ is approximately 0 during the aerosol-cloud interactions (this is assumed in many GCM model calculations). N_c can be derived from τ and r_e as follows. Because

$$\tau=\frac{3}{2}\frac{LWP}{\rho_w r_e}=\frac{3}{2}\frac{(4/3)\pi\bar{r}^3\rho_w Nh}{\rho_w r_e}=2\pi\frac{\bar{r}^3}{r_e}Nh \qquad (3)$$

where droplet radius is averaged over the cloud layer. Using $r_e^3(1-b)(1-2b)=\bar{r}^3$ (Appendix), we have

$$\tau=2\pi r_e^2(1-b)(1-2b)N_c; \qquad (4)$$

and,

$$N_c=\frac{\tau}{2\pi r_e^2(1-b)(1-2b)} \qquad (5)$$

where b is effective variance of cloud droplet size distribution. Aircraft measurements show values of b ranging from 0.111 for fair weather cumulus to 0.193 for stratus [*Hansen*, 1971], implying $r_e=(1.131\text{-}1.264)\,\bar{r}$. Although N is nearly constant throughout a non-precipitating cloud layer, r_e can vary by as much as 50-100%. The expressions above assume that the average value of r_e over the cloud layer is approximated by the value determined near cloud top, which would tend to overestimate r_e, possibly by as much as 20 - 35% [*Nakajima and King*, 1990], and underestimate N_c. Note, however, that an overestimate of the average r_e in the cloud also implies an overestimate of τ that partly offsets the effect of an r_e error on N_c. To further reduce this underestimate, we use $b = 0.193$.

To validate the derived values of N_c from satellite data, in situ measurements during the ASTEX in the region of the Azores in June 1992 [*Albrecht et al.*, 1995] and the intensive field operations (IFO) phase of FIRE in the region of the San Nicolas Island in July 1987 [*Cox et al.*, 1987] are used. During the ASTEX, cloud column droplet concentration N_c can be calculated from measurements of vertical profiles of droplet concentration and cloud geometric thickness. However, in many of the coordinated flights of aircraft with satellite overpasses, unfavored conditions (cirrus, haze, broken stratocumulus clouds) entangle satellite retrievals [*Platnick and Valero*, 1995]. One case (June 12, 1992) is free of these conditions and chosen for our validation purpose. Satellite retrieved optical thickness τ and droplet size r_e [*Platnick and Valero*, 1995] are used to calculate N_c. During the 1987 FIRE IFO, there were no direct measurement of N_c. Therefore, *LWP* and r_e from in situ observations were used to derive N_c by the equation

$$N_c=\frac{3}{4\pi\rho_w}\frac{LWP}{r_e^3(1-b)(1-2b)} \qquad (6)$$

LWP was derived by ground-based microwave observations at San Nicolas Island and the estimated uncertainty is 20% [*Fairall et al.*, 1990]. r_e values were from aircraft in situ measurement using FSSP aboard C130 over stratocumulus during the FIRE campaign [*Rawlins and Foot*, 1990]. Satellite retrievals were based on the data from the ISCCP analysis at individual pixel levels. Only near-nadir viewing pixels are used to avoid possible 3D effects of cloud. During the 1987 FIRE IFO, data from GOES-6 were also used to retrieve cloud properties [*Minnis et al.*,

Table 1. N_c's from satellite and ground measurements

Date	Satellite τ	Satellite r_e (μm)	Satellite N_c (10^6/cm^2)	Ground LWP (g/m^2)	Ground r_e (μm)	Ground N_c (10^6/cm^2)
FIRE						
7/5/87	9.2	8.1	4.5	58.0	7.7	6.1
7/16	13.0	11.2	3.3	60.0	10.0	2.9
7/18	5.0	7.2	3.1	15.0	5.2	5.1
ASTEX				h(m)	N_v (cm^{-3})	
6/12/92	14.8	11.8	3.4	300	150	4.5

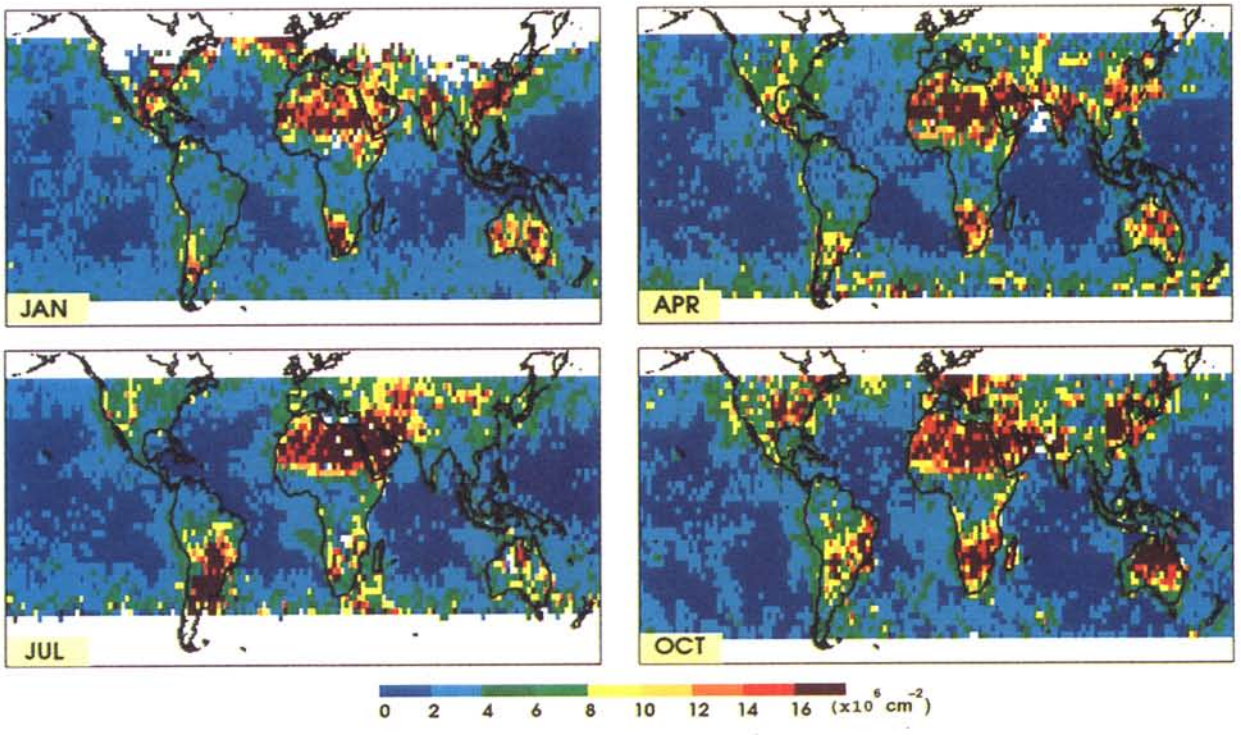

Figure 1. Cloud column droplet concentration retrieved from AVHRR data of NOAA-9, 1987.

1992]. Their results are not used here because it was from a hybrid method, which used ground observed *LWP* to derive cloud droplet sizes. There are three matches of ground-observations with ISCCP results. Table 1 lists the comparison of N_c values derived from satellite retrieval and ground observations. It is readily seen that N_c's derived from both campaigns are the same order as those retrieved from satellite radiance data. The averaged discrepancy between satellite retrievals and in situ measurements from these four cases is a 19% underestimation from results by remote sensing.

3. Results

Figure 1 shows the retrieved values of N_c for January, April, July and October of 1987. The values shown in the figure can be related to volume droplet concentration, N, in cm^{-3} by dividing by a typical cloud layer thickness. Analysis of rawinsonde humidity profiles indicates that cloud layer thicknesses for clouds with tops ≤ 3000 m are mostly less than 800 m [*Poore et al.*, 1995]. For a typical stratocumulus cloud with geometrical thickness of 300 m [e.g., *Cahalan et al.*, 1994], the dark blue color ($N_c < 2 \times 10^6$ cm^{-2}) in Fig. 1 corresponds to volume droplet concentration $N < 67$ cm^{-3}, which is consistent with aircraft measurements in marine clouds (e.g., N is between 30 and 50 cm^{-3} outside of ship tracks [*Radke et al.*, 1989]; between 30 and 100 cm^{-3} for stratiform cloud over the North Pacific [*Albrecht*, 1989]); the brown color ($N_c \geq 16 \times 10^6$ cm^{-2}) corresponds to $N \geq 530$ cm^{-3}. The rawinsonde results also indicate that the systematic variations of cloud layer thicknesses with latitude and between land and ocean are ~ 25%.

The most striking feature in the geographic distribution of N_c is the contrast between maritime and continental clouds: cloud droplet concentrations over continental areas ($N_c > 8 \times 10^6$ cm^{-2} or $N > 160$ cm^{-3}), except over tropical rain forests, are more than two to four times the values in clouds over maritime areas ($N_c < 4 \times 10^6$ cm^{-2} or $N < 80$ cm^{-3}). This feature is more obvious in the histogram of N_c (Fig. 2) for continental and maritime low-level clouds. More than 80% of clouds over oceans in all seasons have $N_c < 4 \times 10^6$ cm^{-2}, while less than 30% of clouds over land have column droplet concentrations this small. This feature is a much more direct indication of the expected effect of higher concentrations of aerosols on clouds over land areas than differences of r_e or cloud albedo [*Han et al.*, 1997].

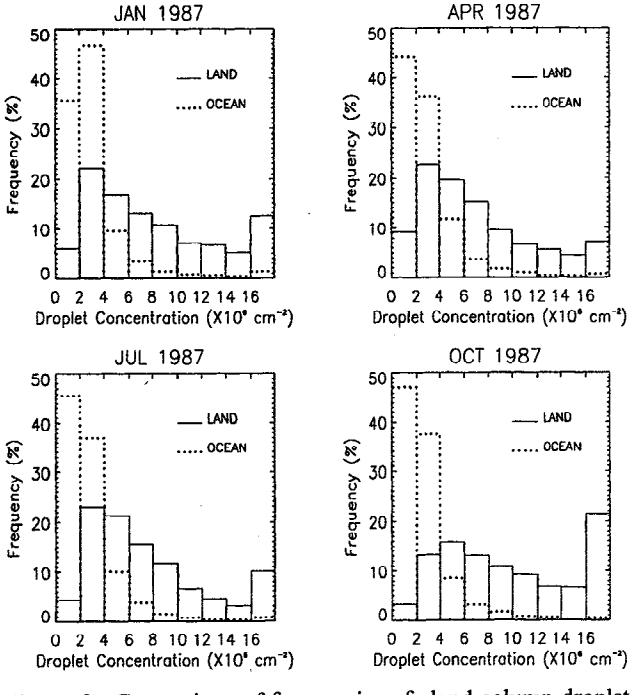

Figure 2. Comparison of frequencies of cloud column droplet concentration for clouds over land and oceans.

Some features in Fig. 1 suggest the effects of anthropogenic aerosol changes, mainly by the release of sulfur dioxide from burning of fossil fuels and of organic and elemental carbon from biomass burning. The seasonal change of N_c over South America is consistent with seasonal variations of biomass burning activities. July and October is the dry season over southern Brazil when biomass burning peaks: values of N_c are often > 300 cm^{-3}. January and April are the wet season and N_c is typically < 100 cm^{-3} over Brazil. The very high N_c values in the Gulf of Mexico, near the east coasts of the U.S. and China, and over western Europe are all consistent with the effect of heavy air pollution from fossil fuel burning.

However, the cause of the moderate-to-high values of N_c in the southern oceans (30°S to 50°S) during April and July is not known. This feature could result from an enhanced CCN concentration arising from DMS production and its oxidation [*Charlson et al.*, 1987]. This possibility is supported by estimates of moderately high primary production (60 - 200 g C m^{-2} yr^{-1}) by marine biology in the zone from 40°S to 60°S [*Berger*, 1989]. The large values of N_c over the Sahara desert all year round could be an artifact because dust storms may be included as clouds in the ISCCP dataset, as also suggested by unusually small values of r_e found in this area [*Han et al.*, 1994]. The small values of N_c over the Rocky Mountains and Gobi desert areas during January and April are associated with unusually large values of r_e that may be caused by thin ice-cloud contamination of these results [*Han et al.*, 1994].

4. Discussion

This first near-global survey of column droplet concentrations (N_c) in low-level (liquid) water clouds clearly shows systematic increases of N_c between regions known to have very low and very high aerosol concentrations. Although the interpretation is obscured somewhat because variations of N_c can be caused by changes of cloud layer thickness, N_c nevertheless captures the changes that are relevant to aerosol effects on cloud albedo. Previous attempts to find an "aerosol effect" on clouds, using either determinations of cloud albedo or droplet size, were difficult to interpret because the liquid water content or liquid water path were also varying [*Han et al.*, 1997]. Variations of N_c more directly show the effects of variations of aerosol concentration: the survey shows the expected variations of the column droplet concentration between continental and maritime clouds and in tropical areas during dry seasons where biomass burning is prevalent. However, to establish and quantify the relation between aerosol concentration and cloud changes, we need to combine the measured changes of N_c and r_e in clouds with changes in the aerosol concentration at a minimum.

Acknowledgments. This research was supported by NASA grant No. NAGW-3788, NAGW-3922 and NAG1-1955; was partially funded by DOE NIGEC through the Great Plains Regional Center (DOE Cooperative Agreement No. DEFC03-90ER61010). The ISCCP international manager is Dr. Robert A. Schiffer. The ISCCP is part of the World Climate Research Program supported by the efforts of several nations.

Appendix: Relationship between r_e^3 and $\bar{r}^3$

Gamma distribution

Assume cloud droplet size distribution follows the gamma distribution $n(r)=cr^{\frac{1-3b}{b}}e^{-\frac{r}{ab}}$, which has the simple properties of r_e=a and v_e=b.

$$\bar{r}^3 = \frac{\int_0^\infty r^3 c r^{\frac{1-3b}{b}} e^{-\frac{r}{ab}} dr}{\int_0^\infty c r^{\frac{1-3b}{b}} e^{-\frac{r}{ab}} dr} = \frac{\Gamma\left(\frac{1}{b}+1\right)\Big/\left(\frac{1}{ab}\right)^{\frac{1}{b}+1}}{\Gamma\left(\frac{1}{b}-2\right)\Big/\left(\frac{1}{ab}\right)^{\frac{1}{b}-2}} = a^3(1-b)(1-2b)$$

Therefore, $r_e^3\,(1-b)(1-2b) = \bar{r}^3$.

Bimodal gamma distribution

For bimodal gamma distribution, we use

$$n(r) = \frac{1}{2}\frac{r^{(1-3b)/b} e^{-r/(a_1 b)}}{(a_1 b)^{(1-2b)/b}\Gamma[(1-2b)/b]} + \frac{1}{2}\frac{r^{(1-3b)/b} e^{-r/(a_2 b)}}{(a_2 b)^{(1-2b)/b}\Gamma[(1-2b)/b]}$$

and it's easy to show that

$r_e = (a_1^3 + a_2^3)/(a_1^2 + a_2^2)$ and $\bar{r}^3 = (a_1^2 + a_2^2)(1-b)(1-2b)r_e/2 = c(1-b)(1-2b)r_e$.

For extreme case, assume $a_2 = 5a_1$ [e.g., *Pruppacher and Klett*, 1978], then $\bar{r}^3 = 0.55(1-b)(1-2b)r_e^3$. This is equivalent to enlarge the value of b, which is why the range of b value of all clouds is larger than that of the gamma distribution. For example, *Fouquart et al.* (1990) derived an equation of $r_e = k(w/\rho N)^{1/3}$, with k values range from 0.62 to 1.02 μm, typical value 0.70 μm, which is equivalent to $r_e^3 = 4k\pi\bar{r}^3/(3\rho) = \bar{r}^3/m$, with m ranging from 1.00 to 0.225, typical value of 0.70. The corresponding form of m for the gamma distribution is $m = (1-b)(1-2b)$. The solution of this equation gives value of b ranging from 0 to 0.33, typical value 0.111.

References

Albrecht, B. A., Aerosols, cloud microphysics and fractional cloudiness. *Science*, **245**, 1227-1230, 1989.

Albrecht, B. A., C. S. Bretherton, D. Johnson, W. H. Scubert, and A. S. Frisch, The Atlantic stratocumulus transition experiment - ASTEX. *Bull. Amer. Meteor. Soc.*, **76**, 889-904, 1995.

Berger, W. H., Global maps of ocean productivity. In: *Berger, W. H., Smetacek, V. S., and Wefer, G. (eds.), Productivity of the Ocean: Present and Past.* Dahlem Konferenzen. John Wiley, Chichester, 429-455, 1989.

Cahalan, R. F., W. Ridgway, W. J. Wiscombe, T. L. Bell, and J. B. Snider, The albedo of fractal stratocumulus clouds. *J. Atmos. Sci.*, **51**, 2434-2455, 1994.

Charlson, R. J., J. E. Lovelock, M. O. Andreae, and S. G. Warren, Oceanic phytoplankton, atmospheric sulphur, cloud albedo and climate. *Nature*, **326**, 655-661, 1987.

Conover, J. H., Anomalous cloud lines. *J. Atmos. Sci.*, **23**, 778-785, 1966.

Cox, S. K., D. S. Modougal, D. A. Randall, and R. A. Schiffer, FIRE- the first ISCCP regional experiment. *Bull. Amer. Meteor. Soc.*, **88**, 114-118, 1987.

Fairall, C. W., J. E. Hare, and J. B. Snider, An eight-month sample of marine stratocumulus cloud fraction, albedo, and integrated liquid water. *J. Climate* **3**, 847-864, 1990.

Fouquart, Y., J.C. Buriez, M. Herman, and R.S. Kandel, The influence of clouds on radiation: A climate-modeling perspective. *Rev. Geophys.*, **28**, 145-166, 1990.

Ghan, S. J., L. R. Leung, R. C. Easter, and H. A. Razzak, Prediction of cloud droplet number in a general circulation model. *J. Geophys. Res.*, **102**, 21777-21794, 1997.

Han, Q., W. B. Rossow, and A. A. Lacis, Near-global survey of effective droplet radii in liquid water clouds using ISCCP data. *J. Climate*, **7**, 465-497, 1994.

Han, Q., W. Rossow, R. Welch, A. White, and J. Chou, Validation of satellite retrievals of cloud microphysics and liquid water path using observations from FIRE. *J. Atmos. Sci.*, **52**, 4183-4195, 1995.

Han, Q., W. B. Rossow, J. Chou, and R. Welch, Global survey of the relationship of cloud albedo and liquid water path with droplet size using ISCCP. [*J. Climate*, In press], 1997.

Hansen, J.E., Multiple scattering of polarized light in planetary atmospheres. Part II: Sunlight reflected by terrestrial water clouds. *J. Atmos. Sci.*, **28**, 1400-1426, 1971.

Hobbs, P.V., L.F. Radke, and S.E.Shumway, Cloud condensation nuclei from industrial sources and their apparent influence on precipitation in Washington State. *J. Atmos. Sci.*, **27**, 81-89, 1970.

Jones, A., D.L. Roberts, and A. Slingo, A climate model study of indirect radiative forcing by anthropogenic sulphate aerosols. *Nature*, **370**, 450-453, 1994.

Lin, B., and W.B. Rossow, Seasonal variation of liquid and ice water path in nonprecipitating clouds over oceans. *J. Climate*, **9**, 2890-2902, 1996.

Martin, G.M., D.W. Johnson, and A. Spice, The measurement and parameterization of effective radius of droplets in warm stratocumulus clouds. *J. Atmos. Sci.*, **51**, 1823-1842, 1994.

Minnis, P., P. W. Heck, D. F. Young, C. W. Fairall, and J. B. Snider, Stratocumulus cloud properties derived from simultaneous satellite and island-based instrumentation during FIRE. *J. Appl. Meteor.*, **31**, 317-339, 1992.

Nakajima, T., and M. D. King, Determination of the optical thickness and effective particle radius of clouds from reflected solar radiation measurements. Part I: Theory *J. Atmos. Sci.*, **47**, 1878-1893, 1990.

Platnick, S., and F. P. J. Valero, A validation of a satellite cloud retrieval during ASTEX. *J. Atmos. Sci.*, **52**, 2985-3001, 1995.

Poore, K., J-H. Wang and W.B. Rossow, Cloud layer thicknesses from a combination of surface and upper air observations. *J. Climate*, **8**, 550-568, 1995.

Pruppacher, H. R., and J. D. Klett, *Microphysics of clouds and precipitation*. Reidel, Dordrecht, Holland, 714pp, 1978.

Radke, L. F., and J. A. Coakley, Jr., M. D. King, Direct and remote sensing observations of the effects of ships on clouds. *Science*, **246**, 1146-1149, 1989.

Raga, G.B., and P.R. Jonas, Microphysical and radiative properties of small cumulus clouds over the sea. *Quart. J. Roy. Meteor. Soc.*, **119**, 1399-1417, 1993.

Rawlins, F., and J. S. Foot, Remotely sensed measurements of stratocumulus properties during FIRE using the C130 aircraft multi-channel radiometer. *J. Atmos. Sci.*, **47**, 2488-2503, 1990.

Rossow, W.B., Cloud microphysics: Analysis of the clouds of Earth, Venus, Mars, and Jupiter. *Icarus*, **36**, 1-50, 1978.

Rossow, W.B., and R.A. Schiffer, ISCCP cloud data products. *Bull. Amer. Meteor. Soc.*, **72**, 2-20, 1991.

Schwartz, S.E., and A. Slingo, Enhanced shortwave cloud radiative forcing due to anthropogenic aerosols. In *NATO ASI Series, V. 135, Clouds, Chemistry and Climate*, P. J. Crutzen and V. Ramanathan (eds.), Springer-Verlag, 191-235, 1996.

J. Chou, Q. Han, and R. M. Welch, Department of Atmospheric Science, University of Alabama in Huntsville, 977 Explorer Blvd. Huntsville, AL 35899. (e-mail: han@atmos.uah.edu)

W. R. Rossow, NASA Goddard Institute for Space Studies, 2880 Broadway, New York, NY 10025.

(Received July 17, 1997; revised January 6, 1998; accepted March 30, 1998)